HHS Public Access

Author manuscript

J Am Soc Mass Spectrom. Author manuscript; available in PMC 2018 November 01.

Published in final edited form as:

J Am Soc Mass Spectrom. 2017 November ; 28(11): 2330–2343. doi:10.1007/s13361-017-1772-2.

Structural Analysis of Unsaturated Glycosphingolipids Using Shotgun Ozone-Induced Dissociation Mass Spectrometry

Rodell C. Barrientos[1], **Ngoc Vu**[1], and **Qibin Zhang**[1,2,*]

[1]Department of Chemistry and Biochemistry, The University of North Carolina at Greensboro, NC 27412 USA

[2]UNCG Center for Translational Biomedical Research, North Carolina Research Campus, Kannapolis, NC 28081 USA

Abstract

Glycosphingolipids are essential biomolecules widely distributed across biological kingdoms yet remain relatively underexplored owing to both compositional and structural complexity. While the glycan head group has been the subject of most studies, there is paucity of reports on the lipid moiety, particularly the location of unsaturation. In this paper, ozone-induced dissociation mass spectrometry (OzID-MS) implemented in a traveling wave-based quadrupole time-of-flight (Q-ToF) mass spectrometer was applied to study unsaturated glycosphingolipids using shotgun approach. Resulting high resolution mass spectra facilitated the unambiguous identification of diagnostic OzID product ions. Using $[M+Na]^+$ adducts of authentic standards, we observed that the long chain base and fatty acyl unsaturation had distinct reactivity with ozone. The reactivity of unsaturation in the fatty acyl chain was about eight-fold higher than that in the long chain base, which enables their straightforward differentiation. Influence of the head group, fatty acyl hydroxylation and length of fatty acyl chain on the oxidative cleavage of double bonds was also observed. Application of this technique to bovine brain galactocerebrosides revealed co-isolated isobaric and regioisomeric species which otherwise would be incompletely identified using contemporary collision-induced dissociation (CID) alone. These results highlight the potential of OzID-MS in glycosphingolipids research, which not only provides complementary structural information to existing CID technique but also facilitates *de novo* structural determination of these complex biomolecules.

Graphical Abstract

*Corresponding author: Qibin Zhang, q_zhang2@uncg.edu.

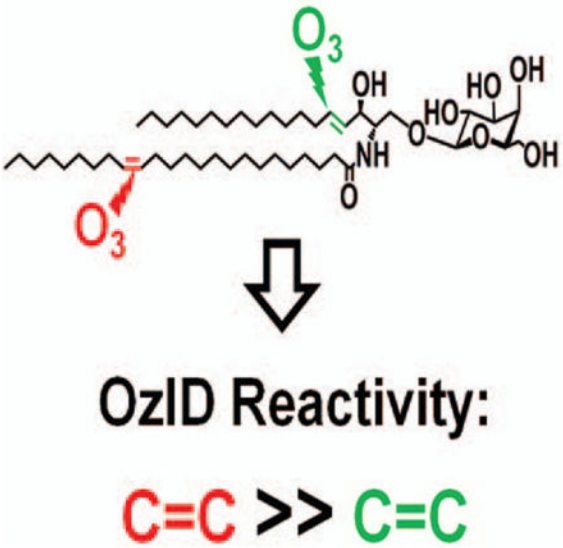

Keywords

Ozone-induced dissociation; glycosphingolipids; cerebrosides; globosides; accurate mass measurement

1. Introduction

Glycosphingolipids are ubiquitous and localize predominantly on the cell surface and some membrane-bound organelles [1–3]. These amphiphilic molecules composed of a glycan head group and ceramide backbone are involved in protein interaction, receptor regulation, initiation and modulation of signal transduction, as well as cell recognition and differentiation [2]. Given these, perturbations in glycosphingolipid metabolism have been recognized as hallmark in a myriad of pathologies including neurological [4, 5], autoimmune [6], and lysosomal storage diseases [7] among others. Recent literature also indicates their potential use as therapeutic agents in cancer and autoimmune diseases due to their immunogenic characteristics [8].

Despite the vast number of studies demonstrating the importance of glycosphingolipids, their structural determination has remained relatively underdeveloped compared to other biomolecules, perhaps due to the various structural complexity arising from the glycan and lipid moieties. The glycan may differ in terms of composition and linkage assignments; whereas for the lipid, the long chain base composition as well as double bond location, and stereochemistry in the fatty acyl chain all can vary [1]. Also, as hydroxylation is prevalent in the fatty acyl chain of these molecules, the presence of this functional group results in the existence of isobaric species thus adding further analytical complexity. While the glycan moiety has been widely studied and possible core structures were identified [1, 3], the lipid backbone is oftentimes overlooked.

Lipid carbon-carbon double bond positional isomers have been shown to possess distinct properties [9]. During biosynthesis, preference for one fatty acid with specific location of unsaturation over the others may reflect normalcy or perturbation of enzymatic activity and metabolic pathways [1, 10]. A wealth of evidences further suggests the importance of unsaturation in the overall attributes of these molecules. Besides its conspicuous effect on membrane fluidity [11], unsaturated glycosphingolipids are also present in specialized tissues/cells such as brain [12], retina[13], and sperm [14] thus indicating that olefin in the lipid backbone is an essential motif for highly specialized biological function. The involvement of lipids and glycolipids as antigens has been demonstrated in prior studies further augmenting the relationship between unsaturation and immunogenic behavior. Specifically, different double bond positions could result in distinct structural conformations thus influencing antigenicity and ultimately, recognition by immune cells [15–19]. Studies also show that some of the potential glycosphingolipid biomarkers of brain development and the underlying diseases are in fact, unsaturated, yet rarely are they identified down to the finest structural detail [12, 20–23]. As such, comprehensive structural determination of intact glycosphingolipids is warranted.

Mass spectrometry (MS) has been the gold standard for rapid determination of glycosphingolipid molecular species [3, 24]. Specifically, gas chromatography-mass spectrometry (GC-MS) was used for a long time to obtain information on both the sequence of the glycan, identity of the fatty acid, and the location of carbon-carbon double bonds after appropriate sample pre-treatment and derivatization [25]. Here, the glycan is typically cleaved off and the lipid backbone is analyzed separately as fatty acid methyl esters, thus losing the intact structural information. Moreover, *de novo* identification of molecular species using this approach is not possible in the absence of an authentic standard. This is particularly important as limited glycosphingolipid standards are currently available commercially [3]. While early studies of intact glycosphingolipids employed fast atom bombardment (FAB) and liquid secondary ion mass spectrometry, these techniques suffer from low sensitivity and complexity of resulting spectra, thus are now largely replaced by soft ionization methods such as electrospray ionization (ESI) [3, 26].

Shotgun MS is a rapid, separation-free approach involving direct infusion of a complex sample commonly using ESI coupled with tandem mass spectrometry (MS/MS) [27]. In the absence of chromatography, isobaric and isomeric species are co-isolated during precursor ion selection, thus, ability to distinguish them in the resulting MS/MS spectrum is necessary. However, structural information obtained using contemporary techniques such as collision-induced dissociation (CID) and higher collision dissociation (HCD) could not distinguish carbon-carbon double bond positional isomers [9, 28, 29]. Although the use of lithiated adducts in ESI-MS/MS of intact glycosphingolipids reveals carbon-carbon double bond location resulting from charge-remote fragmentations [30, 31], oftentimes spectra are complex and difficult to interpret. Similarly, other techniques such as electron capture dissociation (ECD) [32], electron transfer dissociation (ETD) [33], and electron detachment dissociation (EDD) [32], reveal only the complexity of the glycan sequence and the composition of the lipid backbone but the exact location of carbon-carbon double bonds cannot be determined. A number of approaches has been exploited to determine double bond positions in lipids as reviewed by Mitchell and colleagues [34]. More recent approaches

include Paterno-Buchi reaction coupled with MS [35], radical-directed dissociation [36, 37] and ultraviolet photodissociation (UVPD) [38–41]. A simple and economical procedure involving air exposure of lipids on a thin layer chromatography plate followed by ESI-MS analysis could also reveal double bond positions, but data analysis is rather intricate when complex mixture is involved [42].

Ozone (O_3) gas was historically employed to determine carbon-carbon double bond position in glycosphingolipids using in-solution ozonolysis, however the technique is laborious and requires relatively large amount of sample [10]. Harnessing this potential using MS, ozone was generated *in situ* during corona discharge using oxygen as nebulizing gas [43] and later directly employed ozone gas with ESI in a technique called ozone-ESI-MS (OzESI-MS) [44], however, the spectra become increasingly difficult to interpret with increasing sample complexity. Thus, with the advent of ion-molecule reactions, Blanksby and co-workers incorporated ozone gas in an ion trap MS instrument in a technique called ozone-induced dissociation (OzID) [45]. Briefly, in OzID-MS, a precursor ion is mass-isolated followed by selective carbon-carbon double bond reaction with ozone gas which results in formation of characteristic Criegee and aldehyde product ions. The difference in the corresponding mass-to-charge *(m/z)* ratio of the precursor ion and the product ions (neutral losses) are diagnostic of carbon-carbon double bond positions [9]. This simple and rapid technique was successfully implemented in a number of MS platforms [46–50] and applied to characterize isomeric lipids in biological specimens [9, 51].

Recently, we reported the modification and optimization of parameters of a traveling wave-based quadrupole time-of-flight (Q-ToF) mass spectrometer (Synapt™ G2 HDMS, Waters®, UK) to allow the use of ozone as collision gas in the trap and transfer regions [52]. Herein, the said instrument, along with the previously optimized OzID settings [52], was applied to study the fragmentation of glycosphingolipids and demonstrate its capability to differentiate isobaric and isomeric glycosphingolipid species using shotgun approach.

2. Experimental

2.1 Materials

The following standards and natural mixtures were purchased from Avanti Polar Lipids (Alabaster, AL): *D*-lactosyl-β-1,1’ *N*-stearoyl-*D*-erythro-sphingosine (LacCer d18:1/18:0, cat. no. 860598), *D*-lactosyl-β-1,1' *N*-oleyol-*D*-erythro-sphingosine (LacCer d18:1/18:1(9Z), cat. no. 860590), *D*-galactosyl-β-1,1' *N*-oleoyl-*D*-erythro-sphingosine (GalCer d18:1/18:1(9Z), cat. no. 860546), *D*-galactosyl-β-1,1' *N*-stearoyl-*D*-erythro-sphingosine (GalCer d18:1/18:0, cat. no. 860538), *D*-galactosyl-β1-1'-*N*-[2″ (*R*)-hydroxystearoyl]-*D*-erythro-sphingosine (GalCer d18:1/18:0(2OH), cat. no. 860840), *D*-galactosyl-β-1,1' *N*-nervonoyl-*D*-erythro-sphingosine (GalCer d18:1/24:1(15Z), cat. no. 860546) and *D*-glucosyl-β-1,1'N-palmitoyl-*D*-erythro-sphingadiene from soy (GlcCer d18:2 (4*E*,8*Z*)/16:0, cat. no. 131304). Bovine brain galactocerebrosides (cat. no. C4905) was purchased from Sigma (St. Louis, MO). Globotetrahexosylceramide (Gb4Cer d18:1/24:1(15Z)(2ROH), from porcine RBC, cat. no. 1068) and Globotriaosylceramide (Gb3Cer d18:1/18:0, porcine RBC, cat. no. 1529) were obtained from Matreya LLC (State College, PA). All solvents were of LC-MS grade and purchased from Fisher Scientific (Pittsburgh, PA).

2.2 Preparation of standard solutions and natural mixture sample

Standard stock solutions were prepared as 1.0 μg μL^{-1} in chloroform/methanol/water ($CHCl_3$/MeOH/H_2O, 2:1:0.1, *v/v*) and kept at -20°C until further use. Working solutions for direct infusion experiments were made from these solutions by measuring appropriate aliquots in glass vials followed by drying under a stream of nitrogen gas and subsequent reconstitution in acetonitrile/isopropanol/water (ACN/IPA/H_2O, 65/30/10, *v/v*) to a final concentration of 10 pmol μL^{-1}. Soy and bovine brain galactocerebrosides were prepared as 0.01 μg μL^{-1} in ACN/IPA/H_2O, 65/30/10 (*v/v*) from corresponding stock solutions in $CHCl_3$/MeOH/H_2O (2:1:0.1, *v/v*).

2.3 Instrument set-up

The OzID-MS experiments were performed on a modified Synapt™ G2 HDMS instrument (Waters, Manchester, UK) as reported previously [52]. Briefly, O_3 MEGA integrated ozone delivery system (MKS Inc., Andover, MA) was connected to the trap and transfer regions of the instrument through a three-way valve. The ozone generator was operated following manufacturer's instructions and produced consistently 6.0 *wt%* ozone in oxygen at a flow rate of 1.0 slm from high purity oxygen (AirProducts, Indianapolis, IN) at 20 psi, which was used as collision gas in the mass spectrometer at a flow rate of 2.0 mL/min. The resulting pressure in the trap region of Synapt™ G2 was ~9.9 x 10^{-3} mbar. For safety purposes, the remote switch of the ozone generator was interlocked with an ambient ozone monitoring system (Teledyne, San Diego, CA) and programmed to shut-off production when ambient ozone exceeds safe levels. Excess ozone was destroyed on-line using a destruction catalyst (MKS Inc., Andover, MA) that converts ozone to oxygen.

2.4 OzID-MS experiments

Standards and samples were directly infused at 5.0 μL/min using an automated syringe pump. The ESI source conditions were optimized and the final working conditions were set at the following values: polarity, positive; spray voltage, 3.0 kV; sampling cone, 30 to 50 V; extraction cone, 6 V; source temperature, 100 °C; desolvation temperature, 200 °C; cone gas flow, 50 L/h; desolvation gas flow, 500 L/h. Isolation of precursor ions was carried out in the quadrupole at ~ 1Th isolation width (LM =16, HM = 15). All spectra were acquired for 1.0 min at 0.5 s/scan. Traveling wave in the trap and transfer regions were operated at the following settings as optimized previously [52]: Entrance, 5.0 V; Bias, 2.0; Trap DC, 0.2; Exit, 0; trap wave velocity, 8 m/s; wave height, 0.2 V; transfer wave velocity, 247 m/s; wave height, 0.4 V. Default instrument settings for all the remaining parameters were applied. Under these settings, the reaction time between ozone and ions is estimated to be ~16.65 ms [52]. Instrument was calibrated daily in Resolution mode using sodium formate following manufacturer's instructions obtaining less than 0.6 ppm (0.5 mDa) RMS residual mass. To compensate for the fluctuations of the ambient conditions during mass measurement, lock mass corresponding to leucine encephalin (*m/z* 556.2711) was employed. Both the full scan and MS/MS levels were mass-corrected traceable to the reference lock mass using MassLynx v4.1 instrument control software (Waters, Manchester, UK).

2.5 Nomenclature of glycosphingolipid structures

The shorthand notations used in this manuscript were based on the recommendations from the LipidMAPS consortium [53]. The CID-MS/MS fragments were annotated according to Domon and Costello [54], and Ann and Adams [30]. For convenience and intuitive presentation of OzID-MS data, the nomenclature for the position of the carbon-carbon double bond was adopted based on the (*n-x*) system where *x* corresponds to the position of unsaturation from the terminal -CH_3 of the hydrocarbon chain, for instance, double bonds in GalCer d18:1(4*E*)/18:1(9*Z*) are respectively annotated as *n-14* and *n-9*.

3. Results and Discussion

Direct infusion of authentic glycosphingolipid standards yielded predominantly sodiated adducts without addition of sodium ions in solution. Thus, parameters were optimized for $[M+Na]^+$ and used as precursor ion in the succeeding OzID-MS experiments. Of note, no in-source fragmentation was observed in any of our samples parallel to prior investigations involving oligosaccharides which validated the high stability of this adduct [55].

3.1 OzID-MS of common glycosphingolipid long chain bases

Two of the most common long chain bases in glycosphingolipids were chosen to study how these motifs behave in OzID-MS. Specifically, *trans*-4 sphingenine and 4,8-sphingadiene [1, 24, 56].

3.1.1 OzID-MS of long chain base *trans*-4 sphingenine—The most common glycosphingolipid long chain base in mammals is *trans*-4-sphingenine (or simply, sphingosine), designated as d18:1(4*E*) where the double bond is at *n-14* with *trans*-stereochemistry [1, 24, 56]. To determine the behavior of this motif, we first performed OzID-MS of a glycosphingolipid containing saturated fatty acyl chain, GalCer d18:1/18:0(2OH) (Fig. 1a). Two low intensity OzID products, *m/z* 602.3486 (-164 Da) and *m/z* 586.3570 (-180 Da) which differ by 16 Da were observed. Cognizant of alkene OzID-MS reaction pathway proposed previously [9, 45], those two were assigned as Criegee and aldehyde ions, respectively. Interestingly, *m/z* 556.3466 ion was noted which differs by 30 Da from the aldehyde product and is likely resulted from loss of formaldehyde ($H_2C=O$) from *m/z* 586.3570. Although it could also be directly generated from loss of formic acid (HCOOH) from the Criegee ions, its even higher intensity than the Criegee ion suggests that this may not be the case. Elimination of $H_2C=O$ was also observed in phosphatidylcholine-derived Criegee ions as we reported previously due to high proportion of ozone in our measurement conditions [52]. This similar observation might have been due to the structure similarity between the allylic alcohol-derived aldehyde product and the alkene-derived vinyl hydroperoxide (a form of Criegee ion [9]). Moreover, allylic alcohol-derived Criegee ions can exist as a highly unstable vinyl hydroperoxide product which could further rearrange to form ketone group through keto-enol tautomerization (Scheme I). . Of note, loss of $H_2C=O$ was only observed from the cleavage products of the long chain base but not from the fatty acyl double bond (vide infra), indicating the role of allylic hydroxyl group in such elimination process. Aside from these fragments, no other side reactions of ozonolysis was observed. Using accurate mass measurements where ≤5 ppm mass error was consistently

obtained, all OzID-MS product ions and their molecular formula as shown in Table 1 were confidently assigned.

3.1.2 OzID-MS of long chain base 4,8-sphingadiene—The long chain base d18:2(4*E*,8*Z*) also called 4,8-sphingadiene is widespread in plant tissues [1, 57, 58] and less prominent in mammals [56]. We studied commercial soy glucocerebroside mixture using the most abundant species, GlcCer d18:2/16:0(2OH) with $[M+Na]^+$ at *m/z* 736.5330. In OzID-MS, the expected products were observed, at *m/z* 628.3663 (-108 Da) and *m/z* 612.3720 (-124 Da) from the oxidative cleavage of *n-10* double bond followed by *n-14* double bond at *m/z* 558.3257 (-54 Da) with barely detectable Criegee ion at *m/z* 574.3222 (-38 Da) (Fig. 1b and Scheme II). In addition, loss of $H_2C=O$ from this species at *m/z* 528.3139 was detected, similar as what observed for the glycosphingolipid discussed above (Fig. 1a). It is of note that the two double bonds in 4,8-sphingadiene have distinct reactivity toward ozone, with the intensity of OzID products at *n-10* position (*cis*) about tenfold higher than that of OzID products originated from the *n-14* position *(trans)*. Although *trans* alkenes are known to be more reactive towards ozone [49], our observation can be attributed to the distinct electronic and steric influences in these positions that outweigh the contribution of double bond geometric configuration to reactivity.

Sullards and co-workers [57] studied the $[M+Li]^+$ adduct of GlcCer d18:2/16:0(2OH) using FAB-MS and identified the long chain base double bond positions. Specifically, while fragmentation of the intact $[M+Li]^+$ could not directly provide evidence for the precise location of the two double bonds, subjecting the *O* ion (sphingoid base) to fragmentation resulted in characteristic 53 u gap for the Δ^8 double bond. A distonic allylic radical with *m/z* 137.2 diagnostic of the Δ^4 double bond was also apparent indicating that these two double bonds have differential fragmentability. More recently, Ryan *et al.* [40] demonstrated the use of 193 nm UVPD for structural analysis of sphingolipids and showed unique fragments corresponding to cleavage of each double bond in d18:2(4*E*,11*Z*)-sphingadiene. While the two C=C in 4,8-sphingadiene did not show different fragmentation mechanism under OzID, we observed a difference in terms of the double bond reactivity, which is in contrast to the results obtained by Sullards *et al.* [57] and Ryan *et al.* [40], simpler spectra were also obtained and data interpretation is more straightforward making it useful for both mammalian and non-mammalian glycosphingolipids determination.

Both the Δ^4 double bond in *trans-4* sphingenine and 4,8-sphingadiene have different reactivity toward ozone than that in alkenes. Zhou and colleagues [42] observed attenuated reactivity of the sphingosine double bond towards oxidation with ozone and singlet oxygen, and rationalized it is due to the electron-withdrawing inductive effect by allylic hydroxyl. This was further supported by recent studies on the free radical-induced oxidation of glycosphingolipids [59, 60]. This explanation is consistent with solution-phase ozonolysis of alkenes which showed the electrophilic nature of ozone in the upstream Criegee mechanism [61]. Conversely, gas phase ozonolysis of alkenes with allylic hydroxyl group revealed opposite findings, specifically, unsaturated alcohols were found to be more reactive than the corresponding olefinic analogs [62]. In their OzESI-MS experiments with sphingomyelin, another lipid class containing the same sphingosine backbone, Thomas and co-workers [44] hypothesized that its gas phase conformation permits hydrogen bonding of the cation in the

headgroup to the allylic hydroxyl of sphingosine thus impairing ozone's access to the double bond. Altogether, these explanations suggest that the peculiar attribute of sphingosine double bond towards oxidation cannot be rationalized in terms of electronic effects of the α-hydroxyl group alone but rather in conjunction with steric contribution by the head group as a result of its gas phase conformation. Our observation is in agreement with these previous studies [42, 44, 59–61].

3.1.3 Influence of head group on the cleavage of long chain base double bond—The proximity of unsaturation in the long chain base to the head group prompted us to study the influence of the glycan on double bond oxidative cleavage. While epimeric sugars glucose and galactose did not show significant difference in OzID-MS features (data not shown), overall, the number of glycan in the head group appeared to influence the reactivity of the sphingosine double bond. Shown in Fig. S1 are the OzID-MS spectra of glycosphingolipids containing one (GalCer) to three (globotriaosyl ceramide, Gb3) sugar moieties. Notably, the intensity of the ozonide ion along with the OzID diagnostic products is increased with increasing number of sugars. This shows that the head group indeed affects the gas phase ozonolysis of lipids either by influencing electronic density distribution in the proximal double bond as a consequence of gas phase conformation [44] or through its direct involvement in the overall reaction mechanism as recognized previously in other lipid classes [45]. Such concepts require further experimental and computational studies to elucidate the overall mechanistic process. Nevertheless, as diagnostic OzID products are conspicuous despite varying glycan lengths, this technique is undoubtedly applicable to more complex glycosphingolipids.

3.1.4 Influence of fatty acyl hydroxylation on the cleavage of long chain base double bond—Both samples described in Fig. 1 possess α-hydroxyl group on the fatty acyl, although the effect is not drastic, its presence appeared to influence the oxidative cleavage of the double bond in the backbone. When GalCer d18:1/18:0(2OH) and GalCer d18:1/18:0 (Fig. S2) were compared, about fivefold enhancement of signal intensity of ozonide and aldehyde products and increased intensity ratio of the OzID diagnostic ions to ozonide were observed. This shows that even with the remoteness of the hydroxy group from the double bond, notable influence is apparent.

Taken together, even though the simplified reaction pathways depicted in Schemes I and II clearly illustrate the overall gas phase ozonolysis process, the reaction mechanism might be more complex as we observed that the head group and the remote functional groups also influence the overall steric as well as electronic environment of the double bond. As also acknowledged in the past [45], these effects, although currently still not quantitative, when carefully considered, could hint on the local environments of the double bond and facilitate glycosphingolipid structural characterization.

3.2 OzID-MS of glycosphingolipid with unsaturated fatty acyl chain

3.2.1 Comparison between long chain base and fatty acyl unsaturation—Glycosphingolipid containing unsaturated fatty acyl chain was investigated using the $[M+Na]^+$ (*m/z* 910.6234) of standard LacCer d18:1/18:1(9Z). As expected, the Criegee and

aldehyde products from *n-9* double bond in the fatty acyl chain were observed at *m/z* 816.4754 (−94 Da) and *m/z* 800.4792 (−110 Da), respectively (Fig. 2a). Owing to the two double bonds present, another set of OzID products was identified characteristic of the *n-14* sphingosine double bond (Criegee ion *m/z* 636.2518 and aldehyde ion *m/z* 620.2554) along with a loss of $H_2C=O$ (*m/z* 606.2396 and *m/z* 590.2464) as discussed earlier. Here the presence of two pairs (m/z 636.2518 and m/z 606.2396, m/z 620.2554 and m/z 590.2464) and the consistent intensity ratio within each pair further suggests that $H_2C=O$ loss from both the aldehyde and Criegee ions is the most probable reaction pathway. It is of note that ions corresponding to fatty acyl double bond were about eight times higher than those of long chain base double bond. Also interestingly, instead of having the anticipated neutral loss of 180 Da and 164 Da directly from the precursor ion, these neutral losses were observed from the OzID products of the fatty acyl double bond. This suggests that oxidative cleavage of these olefins is a non-concerted process, and fatty acyl chain double bond cleavage precedes that of sphingosine analogous to observations with GlcCer d18:2/16:0(2OH) as discussed above (Fig. 1b). The relatively low reactivity of this sphingosine double bond towards oxidation as observed before [42, 44, 59, 60] and in this study, may explain why the unsaturation in the fatty acyl chain is preferentially cleaved off prior to that of the sphingosine. In this respect, Thomas and colleagues performed OzESI-MS of analogous compound sphingomyelin d18:1/18:1(9Z), and showed that only the fatty acyl double bond is prominent [44]. In contrast, our results show the presence of the oxidative cleavage products of both double bonds. While the fatty acyl unsaturation is much more reactive, the difference of reactivity between long chain base double bond and ozone observed by them and us may stem from the different concentrations of ozone used and the different efficiency of OzID reaction in the two OzID-MS instrument platforms. Sequential cleavage of double bonds in OzID-MS of different radyls in phosphatidylcholine was also observed by Poad and co-workers [50].

Shown in Fig. 2b is the OzID-MS of *m/z* 912.6370, the $[M+Na]^+$ of LacCer d18:1/18:0. The spectrum shows an ion at *m/z* 960.6215 corresponding to the ozonide species, $[M+Na+O_3]^+$. Two OzID products, a low intensity *m/z* 748.4138 (−164 Da) and *m/z* 732.4135 (−180 Da) were observed, assigned as Criegee and aldehyde ions, respectively, along with loss of $H_2C=O$ at *m/z* 702.4041.

In contrast to the saturated analog, a remarkable difference in spectrum was distinguished for LacCer d18:1/18:1(9*Z*) molecule. Specifically, for the unsaturated analog, the precursor ion is almost completely depletedand the $[M+Na+O_3]^+$ was found to be significantly higher (Fig. 2a) than the saturated counterpart (Fig. 2b). In addition, another distinct ion at *m/z* 1006.5942 was observed, albeit low intensity corresponding to $[M+Na+2O_3]^+$. In sum, this reflects the high efficiency of ozonolysis reaction under the employed measurement conditions owing to the high proportion of ozone in the collision gas mixture and the increased ozone contact time due to the traveling wave settings in the trap and transfer regions as reported previously [52]. The greater prevalence of ozonide ion (~3 to 4x higher) in the spectrum of unsaturated glycosphingolipid (Fig. 2a) as compared to the saturated analog (Fig. 2b) can be rationalized in terms of the increased affinity of this molecule to ozone due to the additional double bond in the fatty acyl chain.

The observed discrepancy in terms of the relative reactivity of the fatty acyl chain and the sphingosine double bonds is analytically advantageous and can be used to distinguish unsaturation between the long chain base and the fatty acyl chain. Prior studies on OzID-MS of phospholipids and triacylglycerols successfully utilized sequential CID/OzID experiments in a linear ion trap instrument to assign double bond position on specific radyl chain [45, 47, 48, 51]. On the other hand, for glycosphingolipids, these sequential steps were deemed unnecessary as differentiation of the backbone and fatty acyl chain is readily observable. Also, as sphingosine marker *m/z* 264 is sometimes difficult to observe in CID-MS/MS spectrum, OzID-MS is a facile technique for the rapid identification of this long chain base [63].

Moreover, two sets of OzID-MS products (minor products, labelled with * in Fig. 2a) arising from secondary oxidation cleavages from the ozonide $[M+Na+O_3]^+$ were evident which were not observed in the saturated counterpart (*cf.* Fig. 2b). These minor secondary oxidation products were also detected using analogous instrument in a recent report [50]. The ion with *m/z* 778.3867 is a putative loss of 180 Da from *m/z* 958.6110 (Fig. 2a). Since the intensity of this ion was observed to increase with increasing ozonide intensity, we hypothesized that it could result from the ozonide and that increasing number of sugar moiety would also increase the intensity of this secondary oxidation products which we have indeed confirmed (*see* **Section 3.2.2**). Studies on glycosphingolipids exposed to free radicals in the condensed phase reported potential cleavage of the sugar backbone under oxidizing conditions [59, 60]. Based on this notion, two sources of the observed neutral loss (−180 Da) from secondary oxidation in OzID are plausible, *first* is the loss of sugar moiety, and *second* is the cleavage of the sphingosine double bond. Clarification of this ambiguity was greatly facilitated by accurate mass measurements. In the first case, loss of sugar results to an ion with a molecular formula of $C_{42}H_{77}NO_{10}Na$ (*m/z* 778.5445) and mass error of 202.69 ppm, while the second case gives $C_{34}H_{61}NO_{17}Na$ (*m/z* 778.3837) and a mass error of 3.85 ppm. These results indicate that loss of sugar is unlikely and that the neutral loss of 180 Da from the ozonide results from the cleavage of the sphingosine double bond via secondary oxidation processes. In terms of analytical utility, the low abundance of these secondary products does not complicate data interpretation [50].

3.2.2 Effect of the chain length of unsaturated fatty acyl on OzID product branching—

Comparing different unsaturated standards, interestingly, opposite pattern in the intensity of Criegee and aldehyde ions resulting from fatty acyl double bond was observed between GalCer d18:1/18:1(9*Z*) and GalCer d18:1/24:1(15*Z*). In the former, in terms of intensity, the aldehyde > Criegee ion, whereas in the latter, aldehyde < Criegee ion (Fig. 3a and 3b, in red color). Previously, it was reported that phosphoethanolamine (PE) and phosphatidyl inositol (PI) analogs showed opposite intensity ratio of aldehyde and Criegee ions [45]. That difference was rationalized in terms of the gas phase basicities of the different head groups and possible participation of charge in the reaction mechanism. In our present study, analogous pattern was noted notwithstanding the similarity of the head groups indicating the role of hydrocarbon chains in determining the branching ratio. The difference in OzID product intensities we observed could be attributed to the increased flexibility of the fatty acyl chains thus offering greater chance for the double bond to interact with charge,

which is in agreement with previous findings that charge carrier participates in OzID mechanism [45]. This was further confirmed when the $[M+Na]^+$ of one of the most abundant ion in porcine red blood cell globosides, Gb4Cer d18:1/24:1(2OH), was subjected to OzID-MS. As expected, for the 24:1 fatty acyl chain, intensity of Criegee product is higher than the aldehyde (Fig. 3c). Moreover, secondary oxidation products are also observed in agreement with the ones identified in LacCer d18:1/18:1(9Z) thus confirming that an increase in the number of sugar moiety increases propensity towards side reactions. As these products do not impede data interpretation, the utility of this technique for targeted structural analysis of glycolipids containing longer chain glycans is plausible as demonstrated herein.

One remaining challenge in assigning isomeric unsaturated lipids in general and particularly glycosphingolipids, is the stereochemistry of the double bond. The *cis*- and *trans*- isomers are distinguishable using OzID-MS as previously demonstrated [49, 52] but requires authentic standards to enable unambiguous assignments. For glycosphingolipids, only the *cis*- isomers are currently available.

3.3 Application to bovine brain galactocerebrosides

The analytical utility of OzID-MS for glycosphingolipids was tested by infusing bovine brain galactocerebrosides. The full scan accurate mass spectrum of the mixture is shown in Fig. 4a. Cerebrosides are the simplest yet diverse class of glycosphingolipids with high abundance in the brain and have been implicated in neurodegenerative diseases [64, 65]. The co-existence of isomeric and isobaric galactocerebrosides in this sample makes it an excellent model to demonstrate applicability of OzID-MS in glycosphingolipids. By performing CID-MS/MS of each prominent ion under Argon, we tentatively assigned the identity of each species. Subsequently, OzID-MS was performed by selecting the $[M+Na]^+$ as precursor ion.

3.3.1 OzID-MS of major bovine brain galactocerebroside isomers—The two most abundant galactocerebroside species in bovine brain were *m/z* 832.6644 and *m/z* 848.6597. The CID-MS/MS spectrum of *m/z* 832.6644 showed Y_0 ion at *m/z* 670.61 and Z_0 ion at *m/z* 652.60 as well *m/z* 264.26 diagnostic of the d18:1 long chain base [31, 56, 63, 66]. While important, the latter ion is sometimes hardly observable due to its decreased intensity as the number of glycan head group is increased [63]. The B and C ions corresponding to the sugar head group were also detected (Fig. S3-a). This fragmentation data is consistent with previous observations for GalCer d18:1/24:1 and verified using authentic standard shown earlier.

Subjecting *m/z* 832.6644 to OzID-MS, four distinct pairs of OzID products were found (Fig. 4b). The first pair differs from the precursor ion by 66 Da (*m/z* 766.5445) and 82 Da (*m/z* 750.5499), characteristic of *n-7* double bond. Another pair differs by 94 Da (*m/z* 738.5128) and 110 Da (*m/z* 722.5176) from the precursor ion, indicating that another double bond is present at *n-9* position. Each of these ions is paired with a set of Criegee and aldehyde ions of neutral loss 164 Da at *m/z* 586.3229 and *m/z* 558.2813, and 180 Da at *m/z* 570.3274 and *m/z* 542.2943. The lower intensity of the latter ions signify that these are due to the cleavage of the sphingosine double bonds as discussed earlier. Based on this result, these species were

assigned as regioisomers GalCer d18:1/24:1(17*Z*) and GalCer d18:1/24:1(15*Z*) without ambiguity where only the stereochemistry of the double bond is assumed, consistent with previous findings from GC-MS analysis of bovine brain galactocerebrosides [67, 68]. Using an independent reversed phase liquid chromatography-MS (RPLC-MS) analysis employing a variety of core-shell C_{18} and C_{30} columns, these two isomers were found to be co-eluted (data not shown). Same as observations by Poad and colleagues of co-eluting phosphatidylcholine isomers in RPLC, our result highlights the importance of OzID-MS in revealing isomers that are otherwise non-distinguishable even with upfront chromatographic separation and contemporary fragmentation technique [50].

The CID-MS/MS spectrum of *m/z* 848.6597 is shown in Fig. S3-b, with the Y_0 and Z_0 ions at *m/z* 686.61 and *m/z* 668.59, respectively. Cleavage of amide bond resulted to formation of *m/z* 484.33 was also noted indicative of the presence of an α-hydroxy group. Hsu and Turk [31], and Hunnam and colleagues [63] also observed the formation of this ion characteristic of glycosphingolipids hydroxylated at carbon atom adjacent to amide carbonyl. Based on this, *m/z* 848.6597 was tentatively assigned as GalCer d18:1/24:1(2OH). This ion was subjected to OzID-MS and detected two isomers having one double bond in the fatty acyl chain, one at *n-7* and another at *n-9* as evident by pairs of ions at *m/z* 782.5208 (-66 Da) and *m/z* 754.4910 (-82 Da), as well as *m/z* 766.5267 (-94 Da) and *m/z* 738.4954 (-110 Da) assigned as Criegee and aldehyde ions, respectively (Fig. 4c). The sphingosine double bond (-164Da and -180 Da) was observed at *m/z* 602.3013, 586.3046, 574.2703 and 558.2745 respectively along with loss of $H_2C{=}O$ (30 Da), again with much lower intensity. Taken together, this suggests the presence of two hydroxylated regioisomers, GalCer d18:1/24:1(17*Z*)(2OH) and GalCer d18:1/24:1(15*Z*)(2OH) in the sample where only the stereochemistry of the double bond is assumed.

3.3.2 Differentiation of major isobaric galactocerebroside species in bovine brain—One of the challenges in shotgun lipidomics is the co-isolation of isobaric species. For cerebrosides, the simplest glycosphingolipids, this may be particularly important, for example, in the co-presence of hydroxylated, unsaturated species and its non-hydroxylated, saturated analog. Brain cerebrosides is an excellent model system to show this capability and here, *m/z* 834.6771 and *m/z* 850.6727 were chosen as examples.

In theory, isobaric components can be distinguished at the full scan MS level in high resolution (*'W'*) mode of Synapt™ G2 instrument. Using the *'W'* mode, however, two orders of magnitude decline in signal intensity was observed which would require relatively more concentrated sample. Thus, the Resolution (*'V'*) mode was chosen as a trade-off between sensitivity, mass accuracy, and resolution. At this setting on the average, at most ~20,000 full-width at half maximum (FWHM) resolution was achieved and is inadequate to distinguish GalCer d18:1/23:1(2OH) (sodiated adduct, *m/z* 834.6435) and GalCer d18:1/24:0 (sodiated adduct, *m/z* 834.6793), which requires at least 24,000 FWHM.

The *m/z* 834.6771 was tentatively assigned as GalCer d18:1/24:0 based on characteristic fragments identified in its CID-MS/MS spectrum (Fig. S3-c). In OzID-MS, *first*, the ion at *m/z* 654.4553 (-180 Da) was observed along with a low intensity but distinct Criegee ion at *m/z* 670.4456 (-164 Da) and loss of 30 Da from aldehyde at *m/z* 624.4434, respectively (Fig.

5a). *Second,* two pairs of OzID product ions were recognized corresponding to neutral loss of 66 Da (*m/z* 768.5538) and 82 Da (*m/z* 752.5581), and 94 Da (*m/z* 740.5240) and 110 Da (*m/z* 724.5289) which reveal the presence of regioisomeric *n-7* and *n-9* double bonds. These are paired with another smaller set of Criegee and aldehyde product ions which based on their intensity and accurate mass were identified to correspond to the sphingosine double bond. This indicates that GalCer d18:1/24:0 is co-present with its isobaric analog, GalCer d18:1/23:1(2OH) (Fig. 5b). These data showcase the capability of OzID-MS to distinguish isobaric species that are co-isolated during MS/MS step [45] and whose CID-MS/MS spectrum provides low intensity, thus easily overlooked characteristic fragmentations [63]. The lower intensity of the double bond cleavage products (*n-7, n-9)* compared to precursor ion further suggests the relatively lower concentration of these species compared to ones containing saturated fatty acyl chain. In line with our observations, previous reports indicate GalCer d18:1/23:1(2OH) as a minor constituent in the brain while the GalCer d18:1/24:0 as the more abundant species [67, 68]. Also, early studies on total mammalian brain sphingolipids have identified the fatty acyl chain 23:1 with double bond positions at *n-7, n-8, n-9* and *n-10* [10]. In our present study, we only detected *n-7* and *n-9* positions. This implies that these two fatty acyl chains are favored substrates for glycosylation over the others in the downstream biosynthesis of cerebrosides, which indicates that relevant enzymes prefer fatty acyls with specific location of unsaturation. This notion remains a fertile subject of future research.

Another interesting ion, *m/z* 850.6727 was selected for OzID-MS whose spectrum is shown in Fig. 5c. Based on CID-MS/MS pattern (Fig. S3-d), this ion was tentatively assigned as GalCer d18:1/24:0(2OH). As before, neutral losses of 164 Da and 180 Da were anticipated along with a high intensity precursor ion due to its expected reduced reactivity with ozone. Indeed, intact precursor ion was observed as the base peak along with the neutral losses of 164 Da and 180 Da at *m/z* 686.4421 and *m/z* 670.4476, respectively. Additionally, two pairs of OzID products of low intensity were observed indicative of *n-7* and *n-9* double bond positions (Fig. 5d). For galactocerebroside of mass *m/z* 850.6727, plausible structures could be the ones containing a hydroxyl group and one double bond. Thus, assignment was made as GalCer d18:0/24:1(17*Z*)(2OH) and GalCer d18:0/24:1(15*Z*)(2OH) where the stereochemistry was assumed. Indeed, a very low intensity but distinct fragment ion (*m/z* 430.36) was noted in its CID-MS/MS spectrum confirming the existence of these species (Fig. S3-d). Studies have shown that the sphinganine long chain base (d18:0) in bovine brain sphingolipids is at minimal amount when analyzed by GC following cleavage of the glycan head group [68]. This result clearly highlights the utility of OzID-MS in amplifying the signal of these low-level species and its capability to study intact glycosphingolipids in biological samples.

Taken together, shotgun OzID-MS in conjunction with high resolution and high mass accuracy measurement provides a wealth of information on molecular species that are otherwise hardly achievable using common ion fragmentation tools. Furthermore, as accurate mass measurement is insufficient to distinguish isobaric lipids without adequate resolving power, distinct fragmentations obtained using OzID-MS is a very useful tool for structural elucidation.

4. Conclusion

Ability to distinguish glycosphingolipid long chain base and fatty acyl unsaturation is needed, especially in non-mammalian systems where a variety of long chain bases coexist that differ in the position of unsaturation. In this report, for the first time OzID-MS was applied to characterize the structure of intact unsaturated glycosphingolipids. Using this technique, it was possible to rapidly distinguish regiosomeric species in terms of carbon-carbon double bond position of the long chain base and the fatty acyl chain due to their observed differential ozone reactivity. Due to the influence of head group, α-hydroxylation, and fatty acyl chain length, the subtle reactivity differences on the oxidative cleavage of double bonds provide useful hint on the existence of these molecular features and therefore aid in structural elucidation. Accurate mass measurement in the Q-ToF instrument afforded the assignment of OzID-MS products unambiguously, which greatly facilitated the distinction of isobaric species in a complex mixture in the absence of chromatographic separation. Moreover, the highly efficient ozonolysis reaction in the modified Synapt™ G2 instrument enabled the amplification of signals of low abundant species in a complex sample that otherwise would be obscurely identified using CID-MS/MS alone. This shows that OzID and CID, when used as complementary techniques, would enable more comprehensive and definitive structural characterization of glycosphingolipid molecular species in biological samples.

Supplementary Material

Refer to Web version on PubMed Central for supplementary material.

Acknowledgments

This work was partially supported by the National Institute of General Medical Sciences of the National Institutes of Health grant (GM 104678). The authors thank the Triad Mass Spectrometry Facility at the UNCG Chemistry and Biochemistry Department and Dr. Daniel Todd for help with this work.

References

1. Alfred H, Merrill J. Sphingolipid and Glycosphingolipid Metabolic Pathways in the Era of Sphingolipidomics. Chem Rev. 2011; 111:6387–6422. [PubMed: 21942574]
2. Varki, A., Cummings, R., Esko, J. Cold Spring Harbor Laboratory Press; Cold Spring Harbor, New York: 2009.
3. Farwanah H, Kolter T. Lipidomics of Glycosphingolipids. Metabolites. 2012; 2:134. [PubMed: 24957371]
4. Chan RB, Oliveira TG, Cortes EP, Honig LS, Duff KE, Small SA, Wenk MR, Shui G, Paolo GD. Comparative Lipidomic Analysis of Mouse and Human Brain with Alzheimer Disease. J Biol Chem. 2012; 287:2678–2688. [PubMed: 22134919]
5. Boomkamp, SD., Butters, TD. Glycosphingolipid Disorders of the Brain. Quinn, PJ., Wang, X., editors. Springer; Netherlands, Dordrecht: 2008.
6. Misasi R, Dionisi S, Farilla L, Carabba B, Lenti L, Mario UD, Dotta F. Gangliosides and Autoimmune Diabetes. Diabetes/Metabolism Reviews. 1997; 13:163–179. [PubMed: 9307889]
7. Boutin M, Auray-Blais C. Metabolomic Discovery of Novel Urinary Galabiosylceramide Analogs as Fabry Disease Biomarkers. Journal of The American Society for Mass Spectrometry. 2015; 26:499–510. [PubMed: 25582508]

8. Yu AL, Hung JT, Ho MY, Yu J. Alterations of Glycosphingolipids in Embryonic Stem Cell Differentiation and Development of Glycan-Targeting Cancer Immunotherapy. Stem cells and development. 2016
9. Brown SHJ, Mitchell TW, Blanksby SJ. Analysis of unsaturated lipids by ozone-induced dissociation. Biochimica et Biophysica Acta (BBA) - Molecular and Cell Biology of Lipids. 2011; 1811:807–817. [PubMed: 21571093]
10. Kishimoto Y, Radin NS. Structures of the normal unsaturated fatty acids of brain sphingolipids. Journal of Lipid Research. 1963; 4:437–443. [PubMed: 14168187]
11. Stillwell W. The role of polyunsaturated lipids in membrane raft function. Scandinavian Journal of Food and Nutrition. 2006; 50:107–113.
12. Sarbu M, Robu AC, Ghiulai RM, Vukelić Ž, Clemmer DE, Zamfir AD. Electrospray Ionization Ion Mobility Mass Spectrometry of Human Brain Gangliosides. Analytical Chemistry. 2016; 88:5166–5178. [PubMed: 27088833]
13. Brush RS, Tran JTA, Henry KR, McCellan ME, Elliott MH, Mandal MNA. Retinal Sphingolipids and Their Very-Long-Chain Fatty Acid–Containing Species. Invest Ophthalmol Vis Sci Data. 2010; 51:4422–4431.
14. Sandhoff R, Geyer R, Jennemann R, Paret C, Kiss E, Yamashita T, Gorgas K, Sijmonsma TP, Iwamori M, Finaz C, Proia RL, Wiegandt H, Gröne HJ. Novel Class of Glycosphingolipids Involved in Male Fertility. Journal of Biological Chemistry. 2005; 280:27310–27318. [PubMed: 15917254]
15. Kiarash A, Boyd B, Lingwood CA. Glycosphingolipid receptor function is modified by fatty acid content. Verotoxin 1 and verotoxin 2c preferentially recognize different globotriaosyl ceramide fatty acid homologues. Journal of Biological Chemistry. 1994; 269:11138–11146. [PubMed: 8157640]
16. De Libero G, Mori L. How T lymphocytes recognize lipid antigens. FEBS Letters. 2006; 580:5580–5587. [PubMed: 16949584]
17. Yu KOA, Im JS, Molano A, Dutronc Y, Illarionov PA, Forestier C, Fujiwara N, Arias I, Miyake S, Yamamura T, Chang YT, Besra GS, Porcelli SA. Modulation of CD1d-restricted NKT cell responses by using N-acyl variants of α-galactosylceramides. Proceedings of the National Academy of Sciences of the United States of America. 2005; 102:3383–3388. [PubMed: 15722411]
18. Mahfoud R, Manis A, Lingwood CA. Fatty acid-dependent globotriaosyl ceramide receptor function in detergent resistant model membranes. Journal of Lipid Research. 2009; 50:1744–1755. [PubMed: 18716315]
19. Watkins, Erik B., Gao, H., Dennison, Andrew JC., Chopin, N., Struth, B., Arnold, T., Florent, JC., Johannes, L. Carbohydrate Conformation and Lipid Condensation in Monolayers Containing Glycosphingolipid Gb3: Influence of Acyl Chain Structure. Biophysical Journal. 2014; 107:1146–1155. [PubMed: 25185550]
20. Schiopu C, Vukelic Z, Capitan F, Kalanj-Bognar S, Sisu E, Zamfir AD. Chip-nanoelectrospray quadrupole time-of-flight tandem mass spectrometry of meningioma gangliosides: a preliminary study. Electrophoresis. 2012; 33:1778–1786. [PubMed: 22740466]
21. Serb AF, Sisu E, Vukelić Ž, Zamfir AD. Profiling and sequencing of gangliosides from human caudate nucleus by chip-nanoelectrospray mass spectrometry. Journal of Mass Spectrometry. 2012; 47:1561–1570. [PubMed: 23280744]
22. Schiopu C, Flangea C, Capitan F, Serb A, Vukelić Ž, Kalanj-Bognar S, Sisu E, Przybylski M, Zamfir AD. Determination of ganglioside composition and structure in human brain hemangioma by chip-based nanoelectrospray ionization tandem mass spectrometry. Analytical and Bioanalytical Chemistry. 2009; 395:2465–2477. [PubMed: 19841910]
23. Ghiulai RM, Sarbu M, Vukelić Ž, Ilie C, Zamfir AD. Early stage fetal neocortex exhibits a complex ganglioside profile as revealed by high resolution tandem mass spectrometry. Glycoconjugate Journal. 2014; 31:231–245. [PubMed: 24658680]
24. Haynes CA, Allegood JC, Park H, Sullards MC. Sphingolipidomics: Methods for the comprehensive analysis of sphingolipids. Journal of Chromatography B. 2009; 877:2696–2708.

25. Gregson, NA. The Extraction and Analysis of Glycosphingolipids. Graham, JM., Higgins, JA., editors. Humana Press; Totowa, NJ: 1993.
26. Levery SB. Glycosphingolipid structural analysis and glycosphingolipidomics. Methods in enzymology. 2005; 405:300–369. [PubMed: 16413319]
27. Blanksby SJ, Mitchell TW. Advances in Mass Spectrometry for Lipidomics. Annual Review of Analytical Chemistry. 2010; 3:433–465.
28. Olling A, Breimer ME, Peltomaa E, Samuelsson BE, Ghardashkhani S. Electrospray ionization and collision-induced dissociation time-of-flight mass spectrometry of neutral glycosphingolipids. Rapid Communications in Mass Spectrometry. 1998; 12:637–645. [PubMed: 9621447]
29. Kirsch S, Zarei M, Cindrić M, Müthing J, Bindila L, Peter-Katalinić J. On-Line Nano-HPLC/ESI QTOF MS and Tandem MS for Separation, Detection, and Structural Elucidation of Human Erythrocytes Neutral Glycosphingolipid Mixture. Analytical Chemistry. 2008; 80:4711–4722. [PubMed: 18491926]
30. Ann Q, Adams J. Structure determination of ceramides and neutral glycosphingolipids by collisional activation of [M + Li]+ ions. Journal of the American Society for Mass Spectrometry. 1992; 3:260–263. [PubMed: 24242949]
31. Hsu FF, Turk J. Structural determination of glycosphingolipids as lithiated adducts by electrospray ionization mass spectrometry using low-energy collisional-activated dissociation on a triple stage quadrupole instrument. Journal of the American Society for Mass Spectrometry. 2001; 12:61–79. [PubMed: 11142362]
32. McFarland MA, Marshall AG, Hendrickson CL, Nilsson CL, Fredman P, Månsson JE. Structural Characterization of the GM1 Ganglioside by Infrared Multiphoton Dissociation, Electron Capture Dissociation, and Electron Detachment Dissociation Electrospray Ionization FT-ICR MS/MS. Journal of the American Society for Mass Spectrometry. 2005; 16:752–762. [PubMed: 15862776]
33. Han L, Costello CE. Electron transfer dissociation of milk oligosaccharides. Journal of the American Society for Mass Spectrometry. 2011; 22:997–1013. [PubMed: 21953041]
34. Mitchell TW, Pham H, Thomas MC, Blanksby SJ. Identification of double bond position in lipids: From GC to OzID. Journal of Chromatography B. 2009; 877:2722–2735.
35. Ma X, Chong L, Tian R, Shi R, Hu TY, Ouyang Z, Xia Y. Identification and quantitation of lipid C=C location isomers: A shotgun lipidomics approach enabled by photochemical reaction. Proceedings of the National Academy of Sciences. 2016; 113:2573–2578.
36. Pham HT, Julian RR. Characterization of glycosphingolipid epimers by radical-directed dissociation mass spectrometry. Analyst. 2016; 141:1273–1278. [PubMed: 26800360]
37. Pham HT, Ly T, Trevitt AJ, Mitchell TW, Blanksby SJ. Differentiation of Complex Lipid Isomers by Radical-Directed Dissociation Mass Spectrometry. Analytical Chemistry. 2012; 84:7525–7532. [PubMed: 22881372]
38. O'Brien JP, Brodbelt JS. Structural characterization of gangliosides and glycolipids via ultraviolet photodissociation mass spectrometry. Analytical chemistry. 2013; 85:10399–10407. [PubMed: 24083420]
39. Morrison LJ, Parker WR, Holden DD, Henderson JC, Boll JM, Trent MS, Brodbelt JS. UVliPiD: A UVPD-Based Hierarchical Approach for De Novo Characterization of Lipid A Structures. Analytical Chemistry. 2016; 88:1812–1820. [PubMed: 26728944]
40. Ryan E, Nguyen CQN, Shiea C, Reid GE. Detailed Structural Characterization of Sphingolipids via 193 nm Ultraviolet Photodissociation and Ultra High Resolution Tandem Mass Spectrometry. Journal of The American Society for Mass Spectrometry. 2017; 28:1406–1419. [PubMed: 28455688]
41. Klein DR, Brodbelt JS. Structural Characterization of Phosphatidylcholines Using 193 nm Ultraviolet Photodissociation Mass Spectrometry. Analytical Chemistry. 2017; 89:1516–1522. [PubMed: 28105803]
42. Zhou Y, Park H, Kim P, Jiang Y, Costello CE. Surface oxidation under ambient air--not only a fast and economical method to identify double bond positions in unsaturated lipids but also a reminder of proper lipid processing. Analytical chemistry. 2014; 86:5697–5705. [PubMed: 24832382]

43. Thomas MC, Mitchell TW, Blanksby SJ. Ozonolysis of Phospholipid Double Bonds during Electrospray Ionization: A New Tool for Structure Determination. Journal of the American Chemical Society. 2006; 128:58–59. [PubMed: 16390120]
44. Thomas MC, Mitchell TW, Harman DG, Deeley JM, Murphy RC, Blanksby SJ. Elucidation of Double Bond Position in Unsaturated Lipids by Ozone Electrospray Ionization Mass Spectrometry (OzESI-MS). Analytical chemistry. 2007; 79:5013–5022. [PubMed: 17547368]
45. Thomas MC, Mitchell TW, Harman DG, Deeley JM, Nealon JR, Blanksby SJ. Ozone-Induced Dissociation: Elucidation of Double Bond Position within Mass-Selected Lipid Ions. Analytical Chemistry. 2008; 80:303–311. [PubMed: 18062677]
46. Kozlowski RL, Mitchell TW, Blanksby SJ. Separation and Identification of Phosphatidylcholine Regioisomers by Combining Liquid Chromatography with a Fusion of Collision- and Ozone-Induced Dissociation. European Journal of Mass Spectrometry. 2015; 21:191–200. [PubMed: 26307699]
47. Kozlowski RL, Campbell JL, Mitchell TW, Blanksby SJ. Combining liquid chromatography with ozone-induced dissociation for the separation and identification of phosphatidylcholine double bond isomers. Analytical and Bioanalytical Chemistry. 2015; 407:5053–5064. [PubMed: 25740545]
48. Pham HT, Maccarone AT, Thomas MC, Campbell JL, Mitchell TW, Blanksby SJ. Structural characterization of glycerophospholipids by combinations of ozone- and collision-induced dissociation mass spectrometry: the next step towards “top-down” lipidomics. Analyst. 2014; 139:204–214. [PubMed: 24244938]
49. Poad BLJ, Pham HT, Thomas MC, Nealon JR, Campbell JL, Mitchell TW, Blanksby SJ. Ozone-Induced Dissociation on a Modified Tandem Linear Ion-Trap: Observations of Different Reactivity for Isomeric Lipids. Journal of the American Society for Mass Spectrometry. 2010; 21:1989–1999. [PubMed: 20869881]
50. Poad BLJ, Green MR, Kirk JM, Tomczyk N, Mitchell TW, Blanksby SJ. High-Pressure Ozone-Induced Dissociation for Lipid Structure Elucidation on Fast Chromatographic Timescales. Analytical Chemistry. 2017; 89:4223–4229. [PubMed: 28252928]
51. Marshall DL, Pham HT, Bhujel M, Chin JSR, Yew JY, Mori K, Mitchell TW, Blanksby SJ. Sequential Collision- and Ozone-Induced Dissociation Enables Assignment of Relative Acyl Chain Position in Triacylglycerols. Analytical Chemistry. 2016; 88:2685–2692. [PubMed: 26799085]
52. Vu N, Brown J, Giles K, Zhang Q. Ozone induced dissociation on a traveling wave high resolution mass spectrometer for determination of double bond position in lipids. Rapid Communications in Mass Spectrometry. In press.
53. Liebisch G, Vizcaíno JA, Köfeler H, Trötzmüller M, Griffiths WJ, Schmitz G, Spener F, Wakelam MJO. Shorthand notation for lipid structures derived from mass spectrometry. Journal of Lipid Research. 2013; 54:1523–1530. [PubMed: 23549332]
54. Domon B, Costello C. A Systematic Nomenclature for Carbohydrate Fragmentations in FAB-MS/MS Spectra of Glycoconjugates. Glycoconjugate J. 1988; 5:397–409.
55. Zaia J. Mass Spectrometry of Oligosaccharides. Mass Spectrom Rev. 2004; 23:161–227. [PubMed: 14966796]
56. Colsch B, Afonso C, Popa I, Portoukalian J, Fournier F, Tabet JC, Baumann N. Characterization of the ceramide moieties of sphingoglycolipids from mouse brain by ESI-MS/MS: identification of ceramides containing sphingadienine. Journal of lipid research. 2004; 45:281–286. [PubMed: 14595000]
57. Sullards MC, Lynch DV, Merrill AH, Adams J. Structure determination of soybean and wheat glucosylceramides by tandem mass spectrometry. Journal of Mass Spectrometry. 2000; 35:347–353. [PubMed: 10767763]
58. Wang RF, Wu XW, Geng D. Two Cerebrosides Isolated from the Seeds of Sterculia lychnophora and Their Neuroprotective Effect. Molecules. 2013; 18:1181. [PubMed: 23344207]
59. Couto D, Melo T, Maciel E, Campos A, Alves E, Guedes S, Domingues MR, Domingues P. New Insights on Non-Enzymatic Oxidation of Ganglioside GM1 Using Mass Spectrometry. Journal of the American Society for Mass Spectrometry. 2016; 27:1965–1978. [PubMed: 27576485]

60. Couto D, Santinha D, Melo T, Ferreira-Fernandes E, Videira RA, Campos A, Fardilha M, Domingues P, Domingues MR. Glycosphingolipids and oxidative stress: evaluation of hydroxyl radical oxidation of galactosyl and lactosylceramides using mass spectrometry. Chemistry and physics of lipids. 2015; 191:106–114. [PubMed: 26315528]

61. Fliszar S, Granger M. Quantitative investigation of the ozonolysis reaction. XI. Effects of substituents in directing the ozone cleavage of trans-1,2-disubstituted ethylenes. Journal of the American Chemical Society. 1970; 92:3361–3369.

62. Grosjean E, Grosjean D. Rate constants for the gas-phase reactions of Ozone with unsaturated Aliphatic Alcohols. KIN International Journal of Chemical Kinetics. 1994; 26:1185–1191.

63. Hunnam V, Harvey DJ, Priestman DA, Bateman RH, Bordoli RS, Tyldesley R. Ionization and fragmentation of neutral and acidic glycosphingolipids with a Q-TOF mass spectrometer fitted with a MALDI ion source. Journal of the American Society for Mass Spectrometry. 2001; 12:1220–1225. [PubMed: 11720398]

64. Boutin M, Sun Y, Shacka JJ, Auray-Blais C. Tandem Mass Spectrometry Multiplex Analysis of Glucosylceramide and Galactosylceramide Isoforms in Brain Tissues at Different Stages of Parkinson Disease. Analytical Chemistry. 2016; 88:1856–1863. [PubMed: 26735924]

65. Couttas TA, Kain N, Suchowerska AK, Quek LE, Turner N, Fath T, Garner B, Don AS. Loss of ceramide synthase 2 activity, necessary for myelin biosynthesis, precedes tau pathology in the cortical pathogenesis of Alzheimer's disease. Neurobiology of Aging. 2016; 43:89–100. [PubMed: 27255818]

66. Shaner RL, Allegood JC, Park H, Wang E, Kelly S, Haynes CA, Sullards MC, Merrill AH. Quantitative analysis of sphingolipids for lipidomics using triple quadrupole and quadrupole linear ion trap mass spectrometers. Journal of Lipid Research. 2009; 50:1692–1707. [PubMed: 19036716]

67. Murata T, Ariga T, Oshima M, Miyatake T. Characterization of trimethylsilyl derivatives of cerebrosides by direct inlet-chemical ionization mass spectrometry. Journal of Lipid Research. 1978; 19:370–374. [PubMed: 650093]

68. Abe T, Norton WT. The characterization of sphingolipids of oligodendroglia from calf brain. Journal of Neurochemistry. 1979; 32:823–832. [PubMed: 430062]

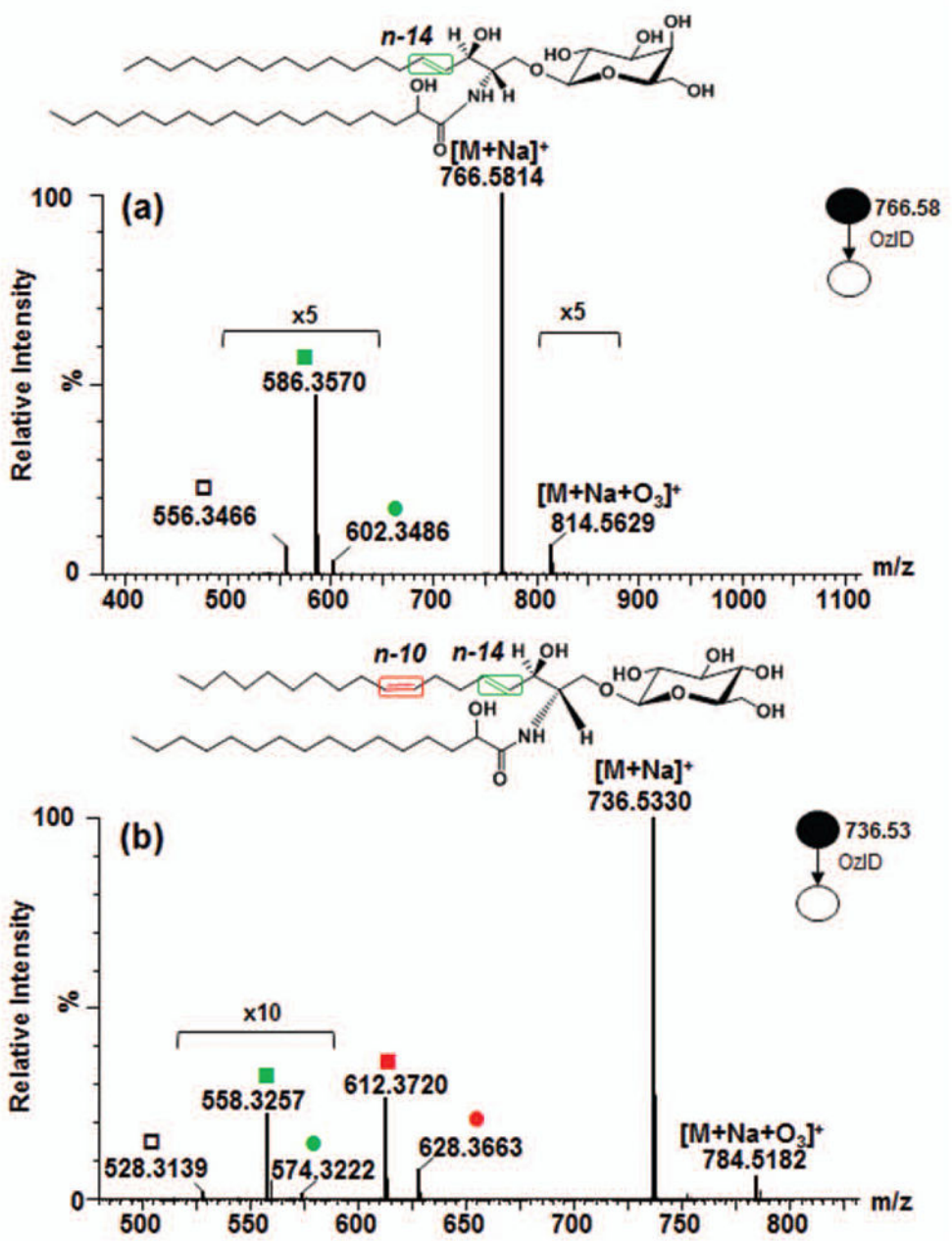

Figure 1.

High resolution OzID-MS spectrum of (**a**) GalCer d18:1/18:0(2OH), and (**b**) GlcCer d18:2/16:0(2OH) standards obtained in Synapt G2™ HDMS. Criegee and aldehyde product ions are depicted as (●) and (■), respectively. Open square (□) indicates ions generated through elimination of $H_2C{=}O$ from the aldehyde ion.

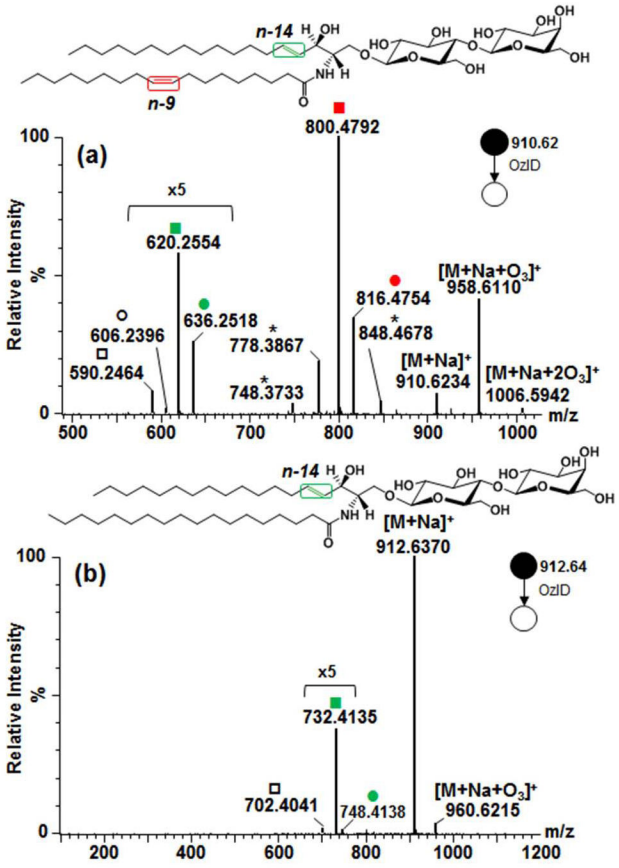

Figure 2.

Comparison of OzID-MS spectra of (**a**) LacCer d18:1/18:1(9Z) and (**b**) LacCer d18:1/18:0. Criegee and aldehyde product ions are depicted as (●) and (■), respectively. Open square (□) and circle (○) indicate ions generated through elimination of $H_2C{=}O$ from the aldehyde ion and Criegee ion, respectively. Asterisk (*) indicates ions generated through secondary oxidation from $[M+Na+O_3]^+$. Colors represent different double bond locations.

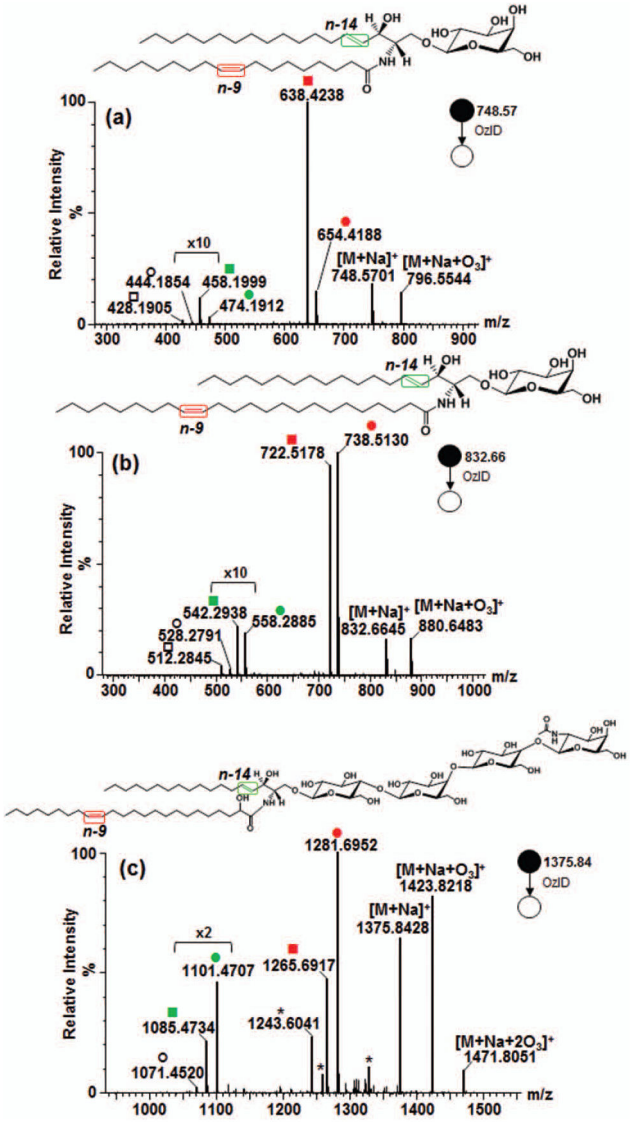

Figure 3.

OzID-MS of (**a**) GalCer d18:1/18:1(9Z), (**b**) GalCer d18:1/24:1(15Z), and (**c**) Gb4Cer d18:1/24:1(15Z)(2OH). (Explanation of symbolic representations is described in Figs. 1 and 2).

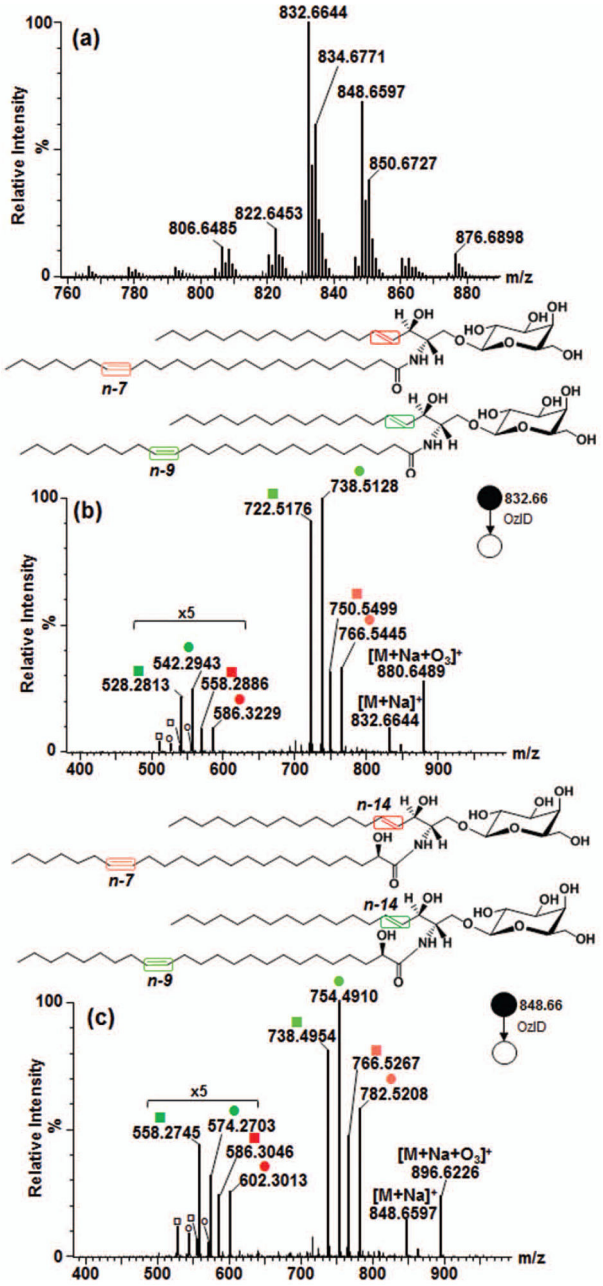

Figure 4.

Application of high resolution OzID-MS to major isomeric galactocerebroside species in bovine brain. **(a)** Full scan MS. **(b)** OzID-MS spectrum of GalCer d18:1/24:1, *m/z* 832.6644 with *n-7/n-14*, and *n-9/n-14* double bonds (fatty acyl chain/long chain base). **(c)** OzID-MS of *m/z* 848.6597 GalCer d18:1/24:1(2OH), with *n-7/n-14*, and *n-9/n-14* double bonds. (Explanation of symbolic representations is described in Figs. 1 and 2).

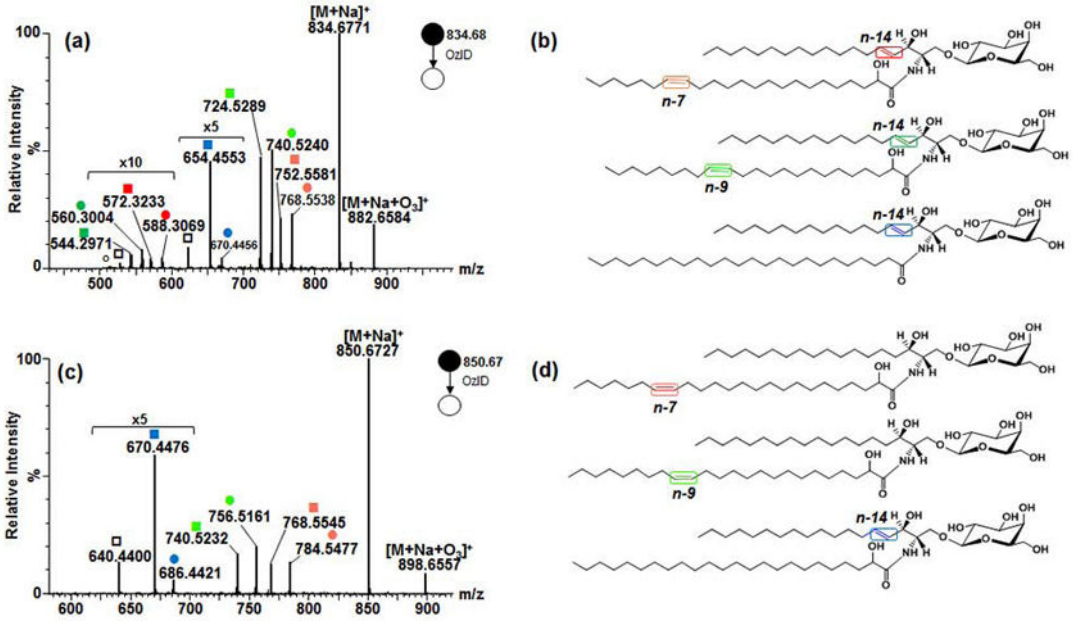

Figure 5.

Application of high resolution OzID-MS to major isomeric and isobaric galactocerebroside species in bovine brain. **(a)** OzID-MS of *m/z* 834.6771 with *n-7*, *n-9* (GalCer d18:1/23:1(2OH)), and *n-14* double bonds (GalCer d18:1/24:0) (**b**). **(c)** OzID-MS spectrum of *m/z* 850.6727 with *n-7*, *n-9* (GalCer d18:0/24:1(2OH)), and *n-14* (GalCer d18:1/24:0(2OH)) double bonds (**d**). (Explanation of symbolic representations is described in Figs. 1 and 2).

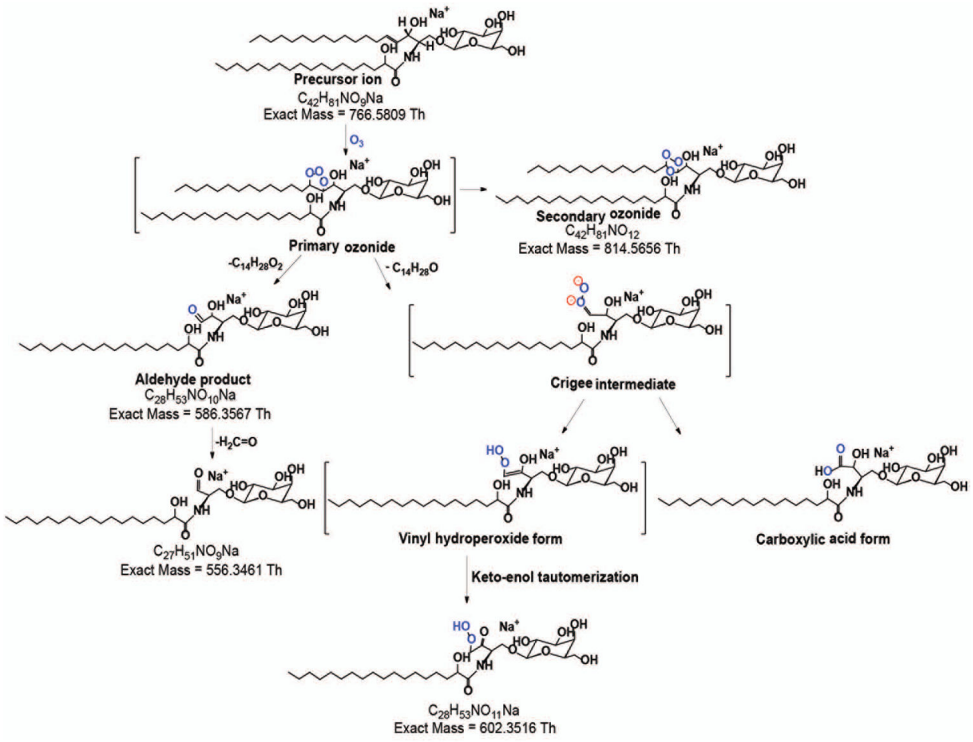

Scheme I.

Proposed reaction pathway for the OzID-MS of the $[M+Na]^+$ of GalCer d18:1/18:0(2OH) (*m/z* 766.5814).

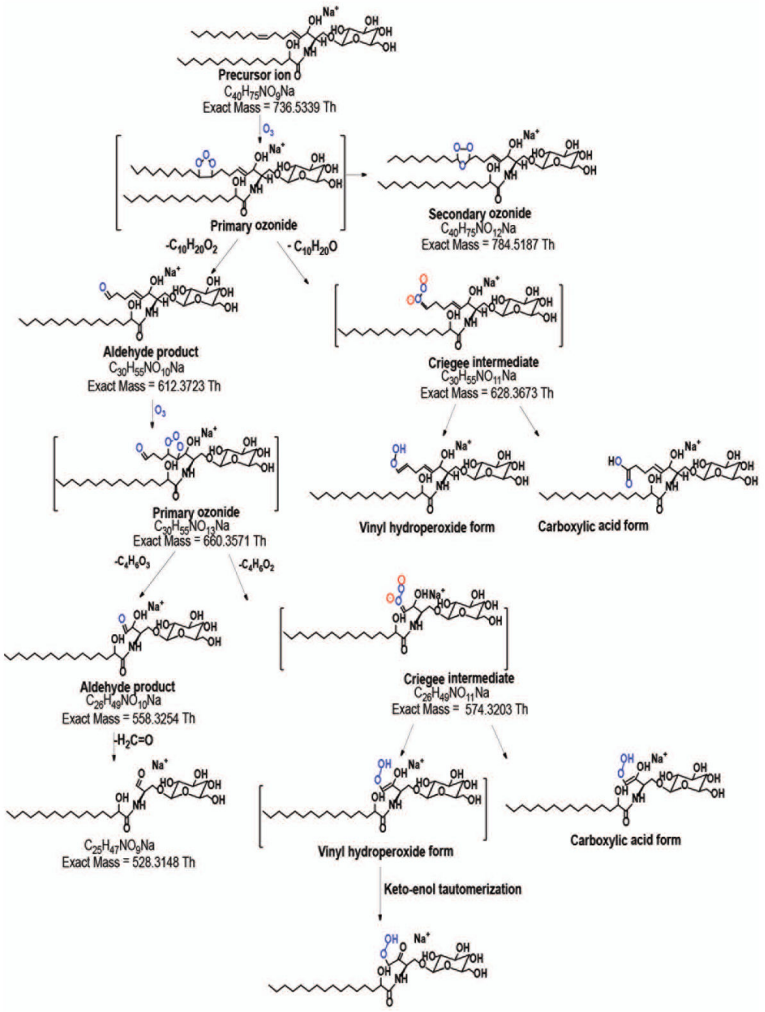

Scheme II.

Proposed reaction pathway for the OzID-MS of the $[M+Na]^+$ of GlcCer d18:2/16:0(2OH) (*m/z* 736.5330).

Table 1

Assignment of OzID-MS product ions based on accurate mass measurement.

Assignment	GalCer d18:1/18:0(2OH)				GlcCer d18:2/16:0(2OH)			
	Molecular Formula	Theoretical Mass (Th)	Observed Mass (Th)	Absolute Error (ppm)	Molecular Formula	Theoretical Mass (Th)	Observed Mass (Th)	Absolute Error (ppm)
$[M+Na+O_3]^+$	$C_{42}H_{81}NO_{12}Na$	814.5656	814.5629	3.34	$C_{40}H_{75}NO_{12}Na$	784.5187	784.5182	0.60
$[M+Na]^+$	$C_{42}H_{81}NO_9Na$	766.5809	766.5814	0.69	$C_{40}H_{75}NO_9Na$	736.5339	736.5330	1.25
Criegee ion *(n-14)*	$C_{28}H_{53}NO_{11}Na$	602.3516	602.3486	5.00	$C_{26}H_{49}NO_{11}Na$	574.3203	574.3222	3.28
Aldehyde ion *(n-14)*	$C_{28}H_{53}NO_{10}Na$	586.3567	586.3570	0.52	$C_{26}H_{49}NO_{10}Na$	558.3254	558.3257	0.54
Criegee ion *(n-10)*	-	-	-	-	$C_{30}H_{55}NO_{11}Na$	628.3673	628.3663	1.53
Aldehyde ion *(n-10)*	-	-	-	-	$C_{30}H_{55}NO_{10}Na$	612.3723	612.3720	0.57
$-H_2C=O$	$C_{27}H_{51}NO_9Na$	556.3461	556.3466	0.84	$C_{25}H_{47}NO_9Na$	528.3148	528.3139	1.77

J Am Soc Mass Spectrom. Author manuscript; available in PMC 2018 November 01.